Carrier doping effect of magnetic and transport properties on the geometrically frustrated iridate Ca5Ir3O12

doi: https://doi.org/10.1016/j.jmmm.2018.12.023

Carrier doping effect of magnetic and transport properties on the geometrically frustrated iridate $Ca_5Ir_3O_{12}$

Sho Haneta[1], Yuki Yasukuni[1], Chiharu Oka[1], Makoto Wakeshima[2], Yukio Hinatsu[2], and Kazuyuki Matsuhira[1]

[1] *Faculty of Engineering, Kyushu Institute of Technology, Kitakyushu, 804-8550, Japan*

[2] *Graduate School of Science, Hokkaido University, Sapporo, 060-0810, Japan*

Abstract

We show the carrier doping effect on magnetic and transport properties of $Ca_5Ir_3O_{12}$, indicating semiconductivity and an antiferromagnetic ordering below Néel temperature $T_N = 7.8$ K. The average valence of Ir ions in $Ca_5Ir_3O_{12}$ is +4.67. Carrier doping for $5d$ electrons of Ir ions is achieved by substitution of Ca^{2+} by Na^+, La^{3+}, and Bi^{3+}; Na substitution leads to hole doping, and La or Bi substitution leads to electron doping. The electrical resistivity decreases in both case of the hole doping or the electron doping. For La10% doped samples, T_N does not change but Curie-Weiss temperature Θ_{CW} becomes 3.5 times larger than 9.9 K for $Ca_5Ir_3O_{12}$. For Bi10% doped samples, T_N decreases to 5 K but Θ_{CW} becomes 3 times larger than that of undoped compound. On the other hand, for Na10% doped samples, T_N decreases to 4 K and Θ_{CW} decreases to 8.3 K. The frustration index f which is defined by $|\Theta_{CW}|/T_N$ is enhanced by electron doping. The magnetic frustration becomes stronger with increase of filling of Ir $5d$ electrons on the triangular lattice.

Keywords:
iridates, frustration, thermoelectric power, resistivity, frustration index

1. Introduction

In recent times, owing to their attractive magnetic and transport properties caused by strong spin-orbit interaction, Ir oxides have attracted enormous attention [1, 2, 3, 4, 5]. In particular, in the case of Ir^{4+} ($5d^5$), the

strong spin-orbit interaction (SOI) splits the sixfold degenerate t_{2g} states into the occupied $J_{\mathit{eff}} = 3/2$ and half-occupied $J_{\mathit{eff}} = 1/2$ states [6, 7]. The $J_{\mathit{eff}} = 1/2$ bands are narrower than the width of the whole t_{2g} band formed in the absence of SOI. Consequently, the system can easily become a Mott-insulating state with even a moderate amount of correlations between the $5d$ electrons. $Ca_5Ir_3O_{12}$, which has a hexagonal structure with space group of $P\bar{6}2m$ (No. 189), exhibits semiconductivity and antiferromagnetic (AFM) ordering below Néel temperature $T_N = 7.8$ K [8, 9, 10, 11]. In recent past, we discovered that $Ca_5Ir_3O_{12}$ along c-axis shows nonlinear conductivity below 300 K [12]. In the crystal structure, one-dimensional (1D) chains of the edge-sharing IrO_6 form triangular lattices. The average valence of Ir ions in $Ca_5Ir_3O_{12}$ is +4.67. In addition, $Ca_5Ir_3O_{12}$ exhibits a second order phase transition at 105 K, where the specific heat shows a sharp anomaly and the electrical resistivity shows a sharp bending. The origin of the phase transition at 105 K is not clear at present, as the structural and magnetic transitions have not been confirmed in X-ray diffraction (XRD), neutron scattering and μSR experiments for the powder samples [9, 11].

In this study, we report the carrier doping effect of magnetic and transport properties on $Ca_5Ir_3O_{12}$. The carrier doping is achieved by substitution of Ca^{2+} by Na^{+}, La^{3+} and Bi^{3+}. Na substitution leads to hole doping for $5d$ electrons, and La or Bi substitution leads to electron doping. As the averaged valence of Ir ions of $Ca_5Ir_3O_{12}$ is +4.67, the ratio between Ir^{4+} and Ir^{5+} is 1/2. For the La10% or Bi10% doped samples, the ratio between Ir^{4+} and Ir^{5+} becomes 1/1. While for Na10% doping, the ratio between Ir^{4+} and Ir^{5+} becomes 1/5. The ratio between Ir^{4+} and Ir^{5+} can be controlled through carrier doping.

2. Experimental Procedures

Polycrystalline sample of $Ca_5Ir_3O_{12}$ and doped (Ca, A)$_5Ir_3O_{12}$ (A = La, Na, and Bi) were synthesized by a standard solid-state reaction. Figure 1 shows the XRD patterns of $Ca_5Ir_3O_{12}$, La10%, Na10% and Bi10%. Similar diffraction patterns from powder XRD measurements are observed. Therefore, the same structure is confirmed for the doped samples. In the XRD pattern of Na10%, small amount of impurity phase (IrO_2) are observed. In the XRD pattern of Bi10%, small amount of the other impurity phase are also observed; we have not been able to identify the impurity phases as this is not a known phase such as $Bi_2Ir_2O_7$ and $CaIrO_3$. The obtained lattice con-

stants of $Ca_5Ir_3O_{12}$, La10%, Na10% and Bi10%, that is obtained by Rietveld analysis [13], are shown in Table 1. Lattice constants varied linearly with the doping amount within 10%. Both lattice parameters of a and c of La10% and Bi10% become larger. The effective ionic radius of La^{3+} and Bi^{3+} is larger than that of Ca^{2+}. The concentration of Ir^{4+} is increased by electron doping. Because the effective ionic radius of Ir^{4+} (0.625 Å) is larger than that of Ir^{5+}(0.57 Å), this result is qualitatively interpreted by electron doping. On the other hand, the lattice parameter a of Na10% becomes slightly larger but the lattice parameter c of Na10% becomes smaller. The effective ionic radius of Na^+ is larger than that of Ca^{2+} but the concentration of Ir^{5+} is increased by hole doping. Therefore, in hole doped samples, there is no significant change of lattice parameters in comparison with electron doped samples.

The electrical resistivity $\rho(T)$ was measured by a four-probe method using Gifford-McMahon refrigerator. The thermoelectric power $S(T)$ was measured by a differential method using a pair of thermocouples (chromel/Au + 7 at% Fe) using self-made ^{4}He cryostat. The DC magnetization $M(H)$ was measured using a SQUID magnetometer (MPMS, Quantum Design, Inc.).

Table 1: Lattice constant a and c, ratio between Ir^{4+} and Ir^{5+}, Curie-Weiss Temperature Θ_{CW}, Néel temperature T_N and frustration index $f = |\Theta_{CW}|/T_N$.

Compound	a (Å)	c (Å)	Ratio (Ir^{4+}/Ir^{5+})	Θ_{CW} (K)	T_N (K)	f
$Ca_5Ir_3O_{12}$	9.4274(4)	3.1950(1)	1/2	-9.9	7.8	1.3
La10%	9.4608(49)	3.2119(12)	1/1	-35	7.8	4.5
Bi10%	9.4477(73)	3.2058(18)	1/1	-29	5.0	5.8
Na10%	9.4315(40)	3.1907(10)	1/5	-8.3	4.0	2.1

3. Experimental Results and Discussion

Figure 2(a) shows the plots of electrical resistivity $\rho(T)$ of $Ca_5Ir_3O_{12}$, La1%, and Na3% as a function of $T^{-1/2}$. $\rho(T)$ for $Ca_5Ir_3O_{12}$ shows clear kink at 105 K, which was previously reported [9]. This anomaly disappears on doping La1% or Na3%. Although the origin of phase transition at 105 K is not clear, this phase transition has the feature that it easily disappears by chemical doping. The phase transition at 105 K is sensitive to chemical

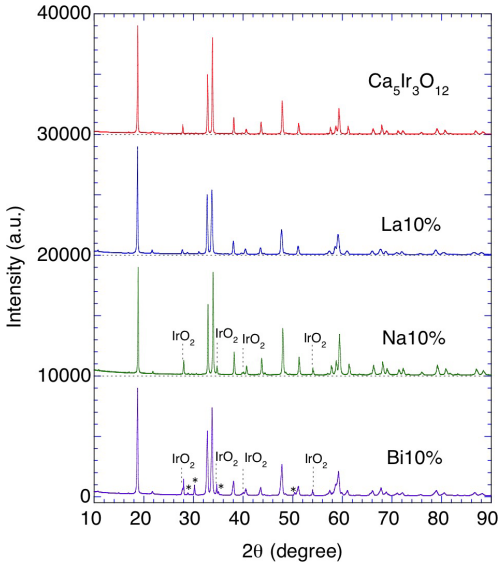

Figure 1: (Color online) XRD patterns of $Ca_5Ir_3O_{12}$, La10%, Na10% and Bi10% that are normalized with respect to the highest intensity. The vertical origins shift to the height indicated by the horizontal broken lines. Asterisk ($*$) indicates peaks impurity phases that are not identified.

composition. As is shown in Fig.2(a), $\ln\rho(T)$ for both $Ca_5Ir_3O_{12}$ and La1% exhibits a $(1/T)^{1/2}$ dependence above 130 K, which is known as variable range hopping (VRH) for 1D systems or Efros-Shkloavskii VRH. However, Na3% does not exhibit a $(1/T)^{1/2}$ dependence, but exhibits a $(1/T)^{1/4}$ dependence (not shown), which is known as VRH for three-dimensional systems. Figure 2(b) shows the electrical resistivities of $Ca_5Ir_3O_{12}$, La10%, Na10%, and Bi10% as a function of T^{-1}. Assuming Arrhenius law at around room temperature, the energy gap for $Ca_5Ir_3O_{12}$, La10%, Na10%, and Bi10% is estimated to be 1139, 1129, 1343, and 545 K, respectively. The energy gap of La10% does not change. The energy gap of Na10% becomes slightly larger. The energy gap of Bi10% is roughly half the value of that for undoped compound. This reduction of energy gap for Bi10% is caused due to the doping of $6s$ electrons from Bi^{3+} which is absent in case of La^{3+}.

Figure 3 shows the temperature dependence of thermoelectric power $S(T)$ of $Ca_5Ir_3O_{12}$, La10%, Bi10%, and Na10%. $S(T)$ of polycrystalline $Ca_5Ir_3O_{12}$ is qualitatively consistent with our result of single crystal. $S(T)$ of La10% shifts toward positive value in the all temperature range. As the energy gap of

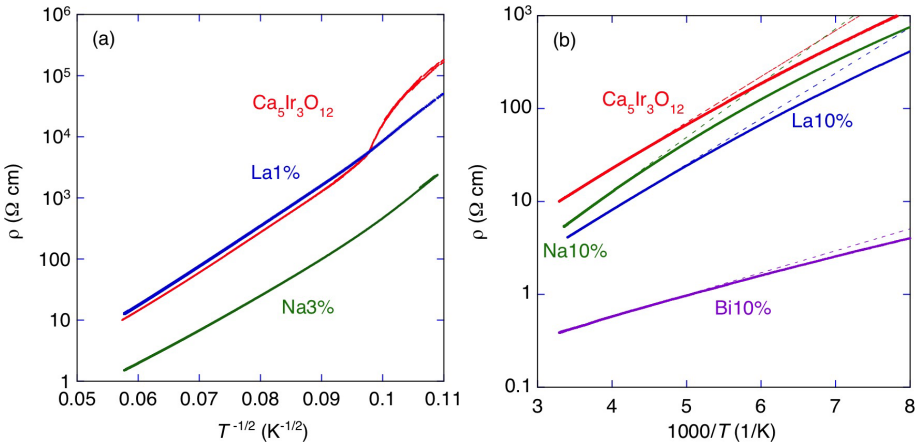

Figure 2: (Color online) (a) Plot of electrical resistivity of $Ca_5Ir_3O_{12}$, La1%, and Na3% as a function of $T^{-1/2}$. (b) Electrical resistivity of $Ca_5Ir_3O_{12}$, La10%, Na10%, and Bi10% as a function of T^{-1}.

La10% is not changed from the result of resistivity, dominant carrier changes from electron to hole. On the other hand, $S(T)$ of Na10% shifts toward negative value. As the energy gap of Na10% becomes larger from the result of resistivity, the electron carrier keeps dominant and carrier number decrease. The sign of $S(T)$ of Bi10% is negative down to 50 K, the absolute value becomes smaller. This result is consistent with the reduction of resistivity by Bi doping.

Figure 4(a) shows the temperature dependence of magnetic susceptibility M/H of $Ca_5Ir_3O_{12}$ and La10%. $Ca_5Ir_3O_{12}$ shows AFM at T_N=7.8 K. M/H measured under zero-field cooled (ZFC) condition shows a sharp peak. The difference in the M/H measured under ZFC and field-cooled (FC) condition observed below T_N, is caused by the canting of AFM coupled moments; the canting moment is considered to be perpendicular to c-axis. As noticed, T_N for La10% is not changed. However, ZFC magnetization shows a kink and the difference between ZFC and FC magnetization is reduced. Figure 4(b) shows the temperature dependence of magnetic susceptibility M/H of $Ca_5Ir_3O_{12}$, Bi10%, and Na10%. ZFC magnetization for Bi10% shows a kink at 5 K and the reduced difference between ZFC and FC magnetization is observed. ZFC magnetization for Na10% has no clear kink. However, a slight difference between ZFC and FC magnetization is observed below 4 K in a magnetic field of 100 Oe (Fig.4(b) inset). We consider that this anomaly is caused by

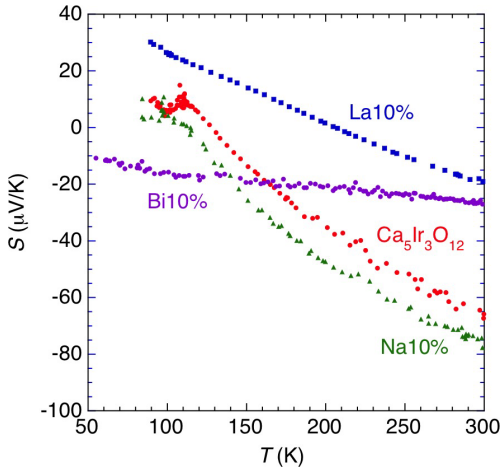

Figure 3: (Color online) Temperature dependence of thermoelectric power of $Ca_5Ir_3O_{12}$, La10%, Na10%, and Bi10%.

AFM ordering; T_N=4 K for Na10%. The difference between ZFC and FC magnetization for all doped samples is reduced significantly. This is due to the vanishing of phase transition at 105 K caused by the carrier doping.

Curie-Weiss Temperature Θ_{CW} for the doped samples is estimated by fitting to the equation $\chi(T) = C/(T - \Theta_{CW}) + \chi_0$; the fittings for undoped sample, La10%, and Na10% were performed for temperatures above 100 K whereas the fitting for Bi10% was performed for temperatures above 50 K. Table 1 shows T_N, Θ_{CW}, and frustration index f which is defined by $|\Theta_{CW}|/T_N$ for La10%, Bi10%, and Na10%; if the value of f is large, a strong magnetic frustration exists in the system. T_N for La10% is not changed but Curie-Weiss temperature Θ_{CW} for La10% becomes 3.5 times larger than the value for the undoped sample. T_N for Bi10% decreases to 5 K but Θ_{CW} for Bi10% becomes 3 times larger than the value for the undoped sample. On the other hand, T_N for Na10% decreases to 4 K and Θ_{CW} decreases from 9.9 K to 8.3 K on Bi10% doping. The frustration index f is enhanced by electron doping. The magnetic frustration becomes stronger due to the electron doping which leads to increasing of $5d$ electrons from Ir. This is a reasonable result because the $5d$ electrons are filled on the triangular lattice by electron doping.

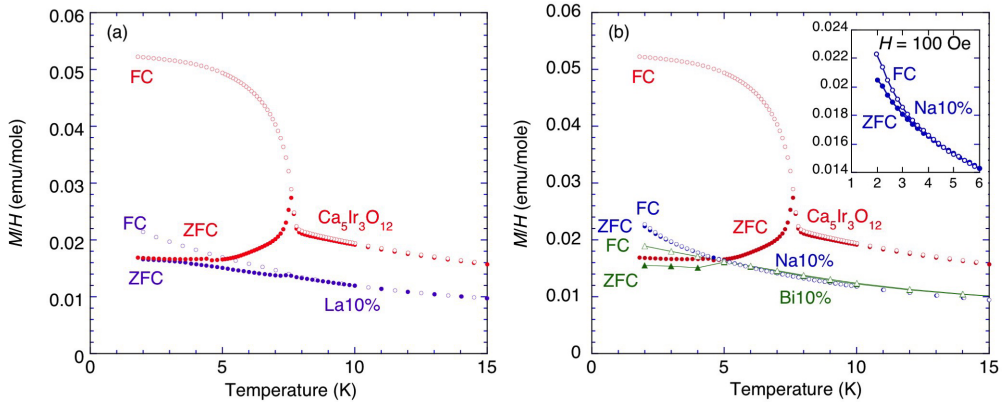

Figure 4: (Color online) Temperature dependence of magnetic susceptibility M/H for (a) $Ca_5Ir_3O_{12}$ and La10% and for (b) for Bi10%, and Na10%. Inset shows M/H of Na10% in a magnetic field of 100 Oe.

4. Summary

We report the carrier doping effect of magnetic and transport properties of geometrically frustrated iridate $Ca_5Ir_3O_{12}$. The carrier doping is performed by substitution of Ca^{2+} by Na^{+}, La^{3+} and Bi^{3+}. Na substitution leads to hole doping, and La or Bi substitution leads to electron doping. The phase transition at 105 K easily disappears on carrier doping and is sensitive to chemical composition. The electron doping (La doping) leads to change the dominant carrier from electron to hole. However, the carrier number and the energy gap, which is estimated by assuming Arrhenius law at around room temperature, does not change. For hole doping (Na doping), the electron carrier remains dominant and the carrier number decrease. The energy gap for Bi10% is roughly a half that for undoped sample. The frustration index f is enhanced by electron doping. The magnetic frustration becomes stronger with increase of filling of Ir $5d$ electrons on the triangular lattice.

5. Acknowledgements

This work was supported by JSPS KAKENHI Grant Number JP18H04327 (J-Physics). This research was partly supported by a Grant-in-Aid for Scientific Research (B) (JP15H03692) from MEXT, Japan. XRD measurements were performed at the Center for Instrumental Analysis in the Kyushu Institute of Technology.

[1] G. Jackeli and G. Khaliullin, Phys. Rev. Lett. **102**, 017205 (2009).

[2] J. Chaloupka, G. Jackeli and G. Khaliullin, Phys. Rev. Lett. **105**, 027204 (2010).

[3] Y. Machida, S. Nakatsuji, Y. Maeno, T. Tayama, T. Sakakibara, S. Onoda: Phys. Rev. Lett. **99**, 037203, (2007).

[4] K. Matsuhira, M. Wakeshima, R. Nakanishi, T. Yamada, A. Nakamura, W. Kawano, S. Takagi and Y. Hinatsu: J. Phys. Soc. Jpn. **76** (2007) 043706.

[5] K. Matsuhira, M. Wakeshima, Y. Hinatsu, and S. Takagi: J. Phys. Soc. Jpn. **80**, 094701 (2011).

[6] B. J. Kim, Hosub Jin, S. J. Moon, J.-Y. Kim, B.-G. Park, C. S. Leem, Jaejun Yu, T. W. Noh, C. Kim, S.-J. Oh, J.-H. Park, V. Durairaj, G. Cao, and E. Rotenberg, Phys. Rev. Lett. **101**, 076402 (2008).

[7] B. J. Kim, H. Ohsumi, T. Komesu, S. Sakai, T. Morita, H. Takagi, T. Arima, Science, **323**, 1329 (2009).

[8] R.F. Sarkozy, W. Moeller, B.L. Chamberland, J. Solid State Chem. **9**, 242 (1974).

[9] M. Wakeshima, N. Taira, Y. Hinatsu, Y. Ishii, Solid State Commun., **125**, 311 (2003).

[10] G. Cao, V. Durairaj, S. Chikara, S. Parkin, and P. Schlottmann, Phys Rev. B, **75**, 134402 (2007).

[11] I. Franke, P.J. Baker, S.J. Blundell, T. Lancaster, W. Hayes, F.L. Pratt, G. Cao, Phys Rev. B, **83**, 094416 (2011).

[12] K. Matsuhira, K. Nakamura, Y. Yasukuni, Y. Yoshimoto, D. Hirai, and Z. Hiroi, J. Phys. Soc. Jpn. **87**, 013703 (2018).

[13] F. Izumi and K. Momma, Solid State Phenom., **130**, 15 (2007).